WWW.IJRPR.COM

International Journal of Research Publication and Reviews

Journal homepage: www.ijrpr.com ISSN 2582-7421

Enhancing the Thermoelectric Properties of Polymers Base Composites

[a]Sidra Jabeen, [b]Dr.Muhammad Sultan, [c]Dr. Malik Sajjad Mehmood

[a,b,c] Department of Physical Sciences, UET Taxila, Pakistan

ABSTRACT

Thermoelectric polymers are a very promising class of thermoelectric materials, is widely used for number of temperature sensitive applications in various industries and clinical laboratories. These are the polymers that have the specific characteristics for the conversion of waste heat into electric energy, however; low conversion efficiency of such polymeric material is the major drawback for such materials.

Polymer base work is focused on studying their improvement in the figure of merit of UHMWPE by adding 10000ppm, 50000ppm, 70000ppm, 100000ppm, 150000ppm, and 200000ppm loadings of grapheme-oxide. The presence of GO and structural stability has been performed while using XRD analysis. For thermoelectric purpose figure of merit has been calculated by using the data of electrical conductivities, Seeback coefficients and thermal conductivities for each formulation. It was found that the value of the figure of merit is 9.97×10^{-11} for 200000ppm loading, which the highest among the all under investigation.

Keywords: PE composites, GO, figure of merit, Thermoelectric characteristics; conductive networks

1. INTRODUCTION

The thermoelectric (TE) process is one of the most promising alternatives for the development of renewable energies and represents one of the most investigated fields to obtain high-efficiency devices for recovery of wasted energy.

The Seebeck effect serves as the foundation for the TE process. When a temperature gradient is applied, charge migration occurs inside the material and an electric potential difference is created. A TE material's efficiency is determined by the so-called figure of merit ZT:

$$ZT = \sigma^* S2 / K$$

where s is the electrical conductivity, S is the Seebeck coefficient, k is thermal conductivity, and T is absolute temperature. The parameter $s*S^2$ is called Power Factor (PF) [1-4]

A TE efficiency of at least 30% is necessary for real-world uses. Nevertheless, there are currently no extremely effective TE materials, and the most cutting-edge research is focused on creating new materials with high ZT.

The semi-conducting system Bi_2Te_3 has the highest ZT at the moment, which is approximately 2. Notwithstanding the benefits of semiconductors, several drawbacks including their high heat conductivity and natural scarcity are essential to their use. Conductive polymers are excellent candidates to replace semiconductors since they have low heat conductivity, in contrast to semiconductors. Furthermore, the materials that make up conductive polymers are readily available, inexpensive, and simple to produce.

To increase a polymer's electrical conductivity and Seebeck coefficient, there are a few primary methods for treating it. One method is to create compounds by adding organic or inorganic fillers to the polymer matrix [4e6]. The insulating PSS portion of some conducting polymers, such as poly(3,4-ethylenedioxythiophene) polystyrene sulfonate (PEDOT:PSS), is adversely influencing the polymer matrix's electrical conductivity. Using various chemical solvents to treat TE material can also improve its characteristics by altering its matrix and causing structural changes. Using polymers or copolymers to treat the primary polymer or to create materials that resemble sandwiches is a third tactic. Numerous studies detail the impact of concurrent treatments on altering the two crucial attributes (i.e. thermal and electrical conductivity) [5-12]

With the ratios of 4:1, 3: 1, 2:1 and 1:1 of polyaniline and graphene nanosheets, respectively, Du et al reported the thermoelectric characteristic of PANI/ GNP for the first time. ZT values, or the figure of merit were discovered to alter for films and pellets from 0.05 to 1.47 and 0.64 to 5.60 $Wm^{-1}k^{-2}$respectively.For the sample comprising 40 weight percent of PANI, Xiang et all's preparation of graphene nanoplatellets (GNP) based polyaniline composites revealed see beck coefficients and electric conductivity values of 33 V/K and 59 S/cm, respectively. This work's primary innovation was the in aniline monomers are polymerized in place for the creation of composites.

More recently, Goa et aldeveloped reduced graphene ABS/r GP nanocomposites by the latex technique using acrylonitrile-butadiene-styrene copolymer. Even though heat conductivity rose with the amount of graphene in ABS grew, electrical conductivity was still discovered to be as high as 0.09 S/m.

This study intends to explore the viability of employing Ultra High Molecular Weight Polyethylene (UHMWPE) a distinctive, industry standard high strength polymer, as a thermoelectric material. Many organic materials with long chains of ethylene monomer (molecular mass varies between 3.5 and 7.5 million amu) have been replaced by UHMWPE because of its abrasion resistance, lack of odour or tasteand non-toxicity. Due to UHMWPE's high molecular weight, it can be produced using powder metal technology and won't modulate, diffuse or stream out as fluid.The characteristics of UHMWPE that encourage its analysis as a subject of interest include its ability to withstand harsh environments, highest heat insulation/absorption capacity among the family, dissipation of energies from various physical processes like stress and pressure etc. Possibility of inducing conducting networks within UHMWPE matrix either by incorporating conductive fillers or by increasing C=C conjugations and most importantly tuning. [13-15]

2. EXPERIMENTAL DETAILS

The topic of preparing and processing our desired sample was covered in this chapter. It also describes each characterisation approach that is necessary for our investigation.

2.1 Synthesis of Graphene Nanoparticle

2.1.1 Preparation of Graphite Electrodes

Get high-quality graphite electrodes first. To assure the creation of high-quality graphene nanoplatelets, electrodes with low impurity contents are essential.

2.1.2 Electrolyte Preparation

Sulfuric acid (H_2SO_4) is used to make the electrolyte solution. To get the appropriate concentration dilute H_2SO_4(0.1mM in deionized water).

2.1.3Electrochemical Cell Setup

Set up a graphite electrode and an electrochemical cell. The electrodes should be positioned parallel to one another and certain distance between them. The exfoliation procedure and the properties of the resultant graphene can be affected by the electrode separation.

2.1.4 Electrochemical Exfoliation

The H_2SO_4 electrolyte solution should be used to submerge the graphite electrodes. Direct current (Dc) of 15 volts should be applied between the electrodes. To guarantee the best exfoliating conditions, the voltage needs to be properly managed. H_2SO_4 is intercalated between the graphite layers during the electrochemical exfoliation process which causes the layers to expand and separate and produce graphene nanoplatelets.

2.1.5 Exfoliation Optimization

Achieve the desired nanoparticles thickness and quality by adjusting the electrochemical parameters such as voltage, electrolyte concentration and exfoliation process. To get the desired outcomes, this phase might need to go through numerous trial cycles.

2.1.6Rinse and Collections

Carefully remove the electrodes from the electrolyte solution after the exfoliating procedure.To get rid of any remaining H_2SO_4 on the graphene nanoplatelets and rinse them with deionized water. Use centrifugation or filtration to remove the nanoplatelets from the remaining H_2so_4.

2.1.7 Drying and Characterization

Using a suitable technique, such as vacuum drying or freeze-drying, dry the gathered graphene nanoplatelets.Once dried, examine the synthesised nanoplatelets shape, thickness and quality employing a range of methods, including Raman spectroscopy and X-ray diffraction (XRD) and other pertinent media.

Figure 1: Prepared GNP

Note: When handling corrosive compounds like H_2SO_4, it is crucial to take the proper precautions such as donning protective gloves, goggles and lab coats. Further guarantees correct chemical disposal and adherence to applicable safety guidelines while carrying out the synthesis procedure.

2.2 Testing and Characterization of GNP

2.2.1 Raman Spectroscopy of GNP

Labram IB dispersive Raman spectroscopy 150m slit, 631.917nm excitation, 2mW, 50 objective, and 600lines/mm diffraction grating were used to perform the Raman spectroscopy. Peltier cooled charge-coupled device detector operating at -40°C for 60 seconds of collection time (10 seconds for silicon).The Raman spectra were moved by 520.7 wave number in order to correct the silicon peak.

The G and two dimensional band shape, location and intensity used for calculate the number of GNP layers in the Raman spectra of GNPs, as shown in Figure 16. As the number of layers rises, the position, width and form of the 2D band altere but G band which is peak position falls lower. GNP peaks are present in the form of D, two dimensional(2D) and G bands at 1350,1550,2650and 1,677 cm^{-1} respectively. The weak and strong D and G peaks (for sp^2 carbon) suggest high sample quality while the broad 2D peak implies multilayer graphite characteristics.[16]

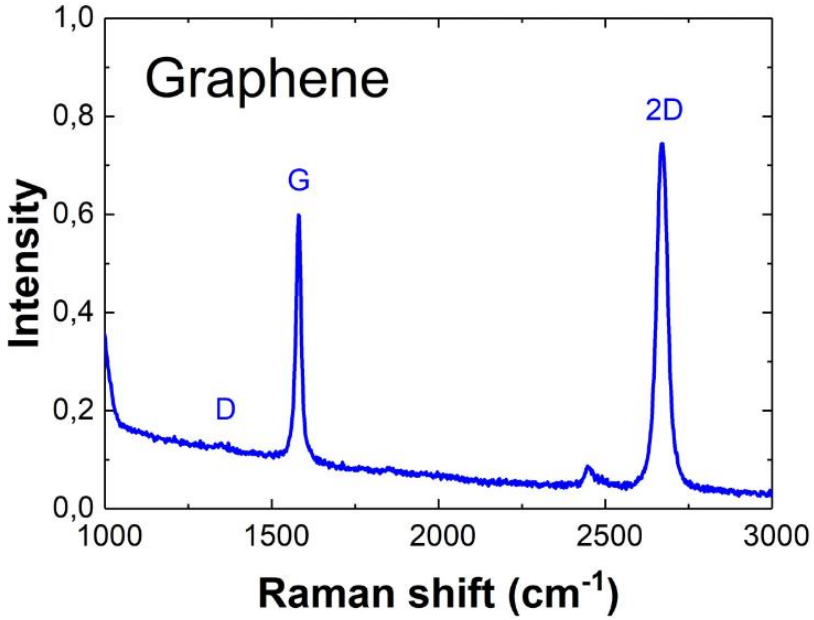

Figure 2: Raman Spectroscopy Graph

The sp^2 carbon atom vibration in the G band Exemplifies a basic graphene band feature. The D band characterizes GNP structural flaws by providing a disordered GNP vibrtional peak.[23] There are well-defined GNPs with minimal flaws. The defect density ratio (nD) and quantity of carbon atoms (nC) is used to compute raman active defect concentrations in ppm(part per million).[24 25]

$$\frac{nD}{nC} = \frac{2.16\times10\text{^}11I(D)}{3.82\times10\text{^}15I(G)} \quad (1)$$

$$nc = 3.82\times10^{15} cm^{-2} \quad (2)$$

The integral area ratio and concentration defects are 0.17 and 10.8, respectively, and I(D) and I(G) are the D and G band integration areas while calculated I(D),/I(G)ratio and GNP defect concentrations compared favorably to graphite and graphene literature values.[17]

3.2.2 X-Ray Diffractometer of GNP

XRD (D8 advance Bruker in Germany), X-ray diffractometer, cu- kα radiation = 0.1541nm, 30Kv,30mA (20-70°,0.02/min scanning speed) was used to establish the GNP purity with the degree of suitability determined by the Bragg R factor, the weighted pattern R factor and the expected R factor. Full prof software and Rietveld pattern analysis were utilized. The optimized sample displacement, peak shape, pattern back drop, preferred orientation, 20 scale factor and parameters(lattice) were used to calculate the GNP crystalline phase abundances. Rietveld improvement was performed using the graphite crystal structures (COD 9000046) and the crystallography open database.

The crystaaline GNP structur's diffraction pattern is displayed in figure 17. Characteristics diffraction peaks with the indices (002), (020), (111) and (004) planes demonstrate the hexagonal crystal structure of GNP without the presence of impurities or second phase peaks. [18]

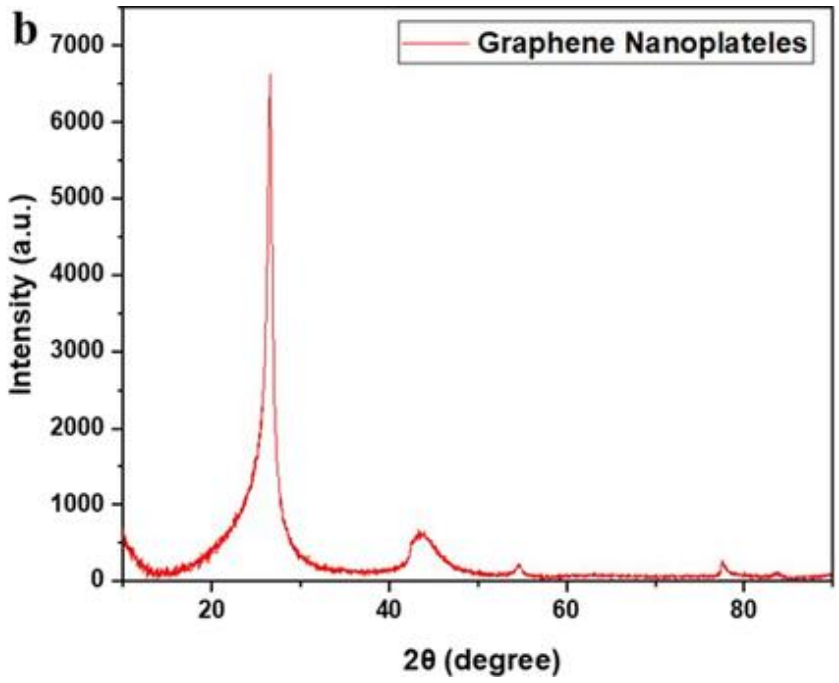

Figure 3 shows the GNP's XRD pattern

The crystallite size is calculated using the reflection profile broadening of XRD pattern and the interlayer spacing is calculated using the matching peak location. The scherrer equation was used to establish the avg crystal size and crystal dimension of GNP and Bragg's Law used to determine the d002(d-spacing for 2H (002) for 2 peak at 25.919°)

$$L_c = \frac{k\lambda}{B\cos\theta} \quad (3)$$

$$d\ 002 = \frac{n\lambda}{2\sin\theta} \quad (4)$$

where X-ray wavelength (0.16419nm), shape factor (0.89), Brag angle and line widening at half the maximal power (maximum radians at half of its width) are represented by K, β, and θ. The calculated crystal size of 13.92nm matched the size of graphite sample determined by Gen et al.[21]The wide (002) resembling reflections physical sources are based on the consistent interlayer spacing (d002) interpretation and are directly connected to average interlayer spacings of 0.335 nm in crystalline graphite, which is indicative of layer misalignment and results match with TEM micrographs. The basal spacing in pure crystalline graphite is the same. Seehra et al. state that the Nc number of layers along the c-axis. [19]

$$Nc = \frac{Lc}{d002} \quad (5)$$

They determined the number of GNP layers by calculating the distance between layers (d002) and apparent crystal size (Lc) in the C-direction. Along the C-axis, there are 43GNP layers.

CRYSTALLITE SIZE

Peak Position (2θ)	FWHM	Lattice Constants (A®)	Average Crystallite size
26.29	0.54831	458.63639	15.54nm

2.3 Preparation and Processing of Samples

2.3.1 Materials

UHMWPE resin powder with an average molecular weight of 3.6107 amu and a density of 0.940/cm^3 was acquired from sigma Aldrich. It also contained 40ml H_2So_4,graphite electrode and 15volt dc power supply. To make UHMWPE/GNP nanocomposites, 1g(Graphite),8ml (H_2So_4) and 25 ml(Water)was utilized.

2.3.2 Preparation of UHMWPE/GNP Composite Pellets

The mixture of GNP and UHMWPE was synthesised with 1wt%, 5wt%, 7wt%, 10wt%, 15wt%, and 20wt% of graphene nanoplatelets to produce the UHMWPE/GNP pellets. Each mixture was combined mechanically for 130 minutes to create the homogeneous mixture using the AIOU mechanical mixer. Each combination was then compressed into pallets with dimensions of 4 mm in thickness and 13 mm in diameter. The AIOU manual laboratory hydraulic press was used to press the materials. Pallet construction involved gradually varying pressures between 50 and 190MPa. Gradually, increased pressure from a low to a high number. 20 mints were given a maximum holding period in order to create compact pallets.

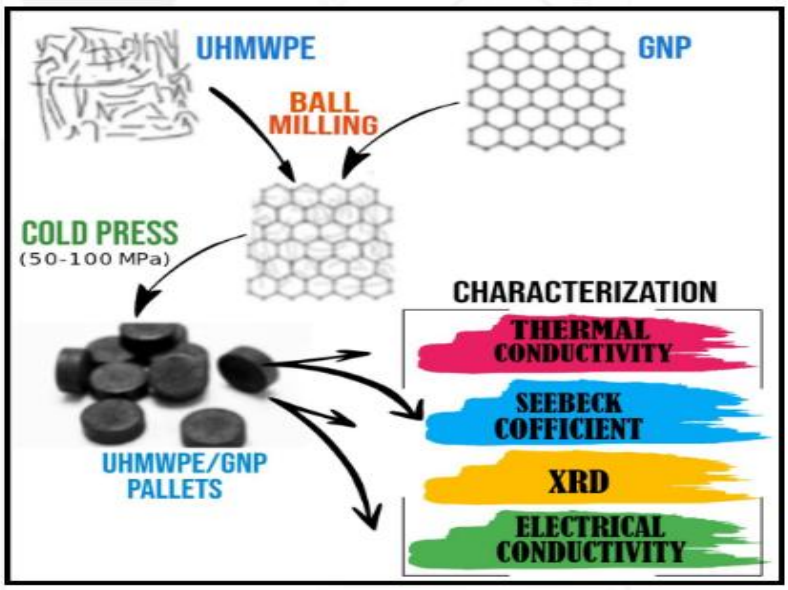

Figure4: Flow chart of experimental setup

2.4 Testing and Characterization of UHMWPE/GNP Pallets

2.4.1 XRD of Pallets

For X-ray diffraction analysis, an X-ray diffracto meter was employed. A current of 40 mA and the instrument's operating voltage of 45 Kv were used. Using the well known Bragg equation and interlayer distance (dhkl) was determined.

$$d_{hkl} = \frac{n\lambda}{sin\theta}$$

Where hkl are the lattice planes and n,θ and λare diffraction level, Bragg's angle and wave length respectively. The X-ray's wavelength was 1.541. From 50 to 600, the reflection mode was used to collect the data and 100 min-1 of scanning was done. The size of average crystallite (D) normal to the lattice plane was calculated using Scherer's formula.

$$D = \frac{K\lambda}{\beta cos\theta}$$

where K is the crystal factor and βis equal to 0.89, and β is the full width at half maxima (FWHM) in radians. The following formula was used to determine the lattice parameter.

$$a = \frac{\lambda}{2sin\theta}\sqrt{h^2 + k^2 + l^2}$$

The following formula was used to determine the nanocomposites' percentage crystallinity.

$$X_c(\%) = \frac{Totalarea - Peakamorphousarea}{Totalarea} \times 100$$

Figure5 : X ray Diffractometer at AIOU

2.4.2 Electrical Conductivity

UHMWPE/GNP composite's electrical conductivity is tested using the four point probe method.The inner two ends yields data on voltage while the outside two ends yield data on current. 4 evenly spaced and material comes into contact with co-linear electrodes made of copper that are placed on a glass substrate to operate it. In addition to length l and cross sectional area A.The following factors determine a composite's electrical conductivity:

$$\sigma = \frac{I}{V} \times \frac{l}{A} = \frac{I}{V} \times \frac{l}{f.w}$$

Where

I= passing of current between the external electrodes

V= measured of voltage at inner electrodes

f= thickness of pallets

w = width of pallets

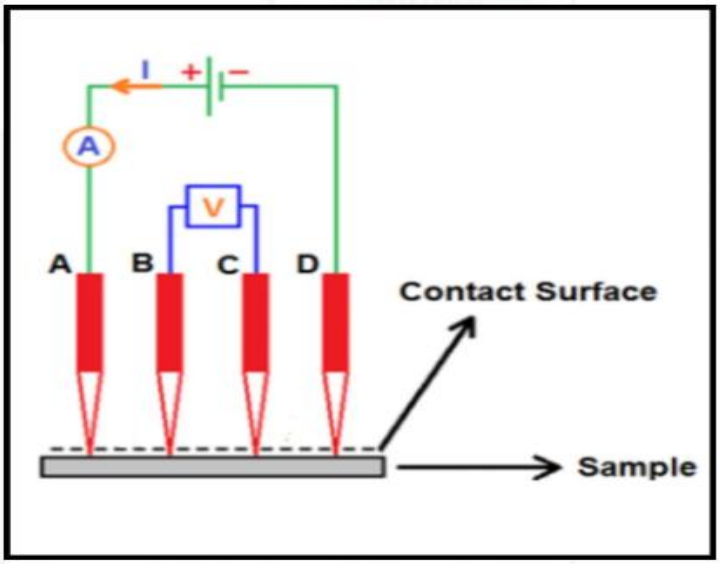

Figure 6: Electrical conductivity setup, Block diagram

23.4.3 Thermal Conductivity

Temperature, chemical composition and microstructures all have an impact on a material's ability to carry out or transmit heat which is known as thermal conductivity. These are full of data testing parameter from microscopic objects. The thermal conductivity of the sample is calculated using the Lee disc method using a steady state methodology.The change in the conditions over a specific period of time is what defines a steady state.i.e when a system is in place or heat enters.

UHMWPE and GNP were positioned on a brass disc. that was covered in a cotton thermal insulator in order to acquire precise readings. The first disc was hot where as the second was not loss heat generation through (a) conduction (b) convection since the air (Atmosphare) might affect producing of results, right insulating material is crucial in getting the right outcomes when Lee's disc is applied. At equilibrium,electric power and heat transfer are equivalent.

Heat Flow Rate(Q) = [$\kappa \times A \times (T_1 - T_2)$] / d

K = Thermal Conductivity (W/mK)

A = *Pellet area*(m^2)

T_1 and T_2 = Temperatures(K)

d = length with which the heat travel (m)

Q = Rate of heat transfer(W)

2.4.4 Seebecki Coefficient

The UHMWPE/GNP composites were given at temperature gradient for seebeck coefficient measurement. By using two different gradient heaters, the pellet's edges was triggered at a greater temperature and other was kept at a lower temperature to accomplish the difference. Voltages were determined through DM5120 (Textronix,) these voltages are essentially seebeck voltages, which was estimated from the sample pellet DTC(Differential thermocouple) by measuring the PD (Potentional difference).

The potential difference between the plates is computed using the Keithley 195A DMM, which was essentially the temperature and voltage. On a power point, these metrics were recorded following the plotting of these reading using software and a plot of V vs T was constructed to obtain the under observation pellet seebeck efficiency.

According to seebeck's assertion, a thermal electric motor field that is calculated using a thermocouple follows a temperature gradient that causes a potential difference. The sample to thermocouple mechanical coupling must be strong enough to achieve accurate counts of voltage and temperature otherwise, it may result in the incorrect seebeck coefficient values. The block graphic below explains the entire scheme condition.

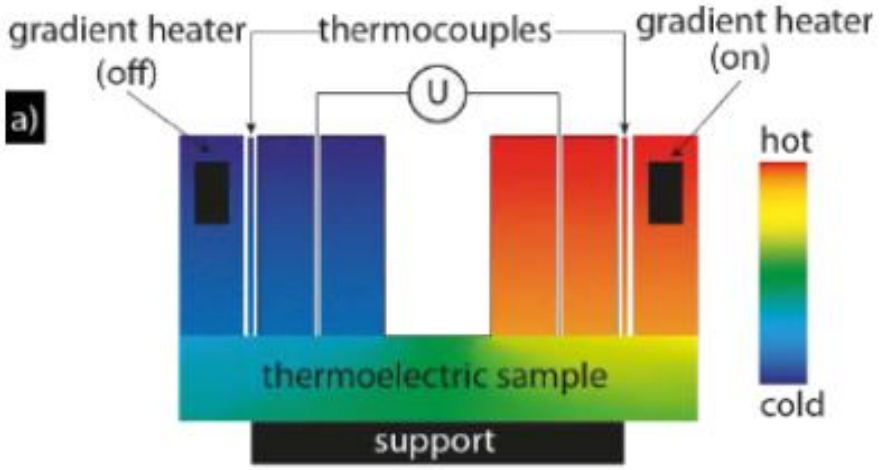

Figure7: See beck effect's block diagram

4. RESULT AND DISCUSSION

The goal of the study was to explore the thermoelectric characteristics of UHMWPE that had been reinforced with various amounts of graphene nanoplatelets. The technique of X-ray diffraction (XRD) was employed for structural examination. For the purpose of calculating the figure of merit for UHMWPE/GNP composites, we discovered the electrical, thermal and Seebeck coefficients.

4.1 Analysis of Structure using X-ray Diffraction

An X-ray diffraction examination has been undertaken prior to examination of the effects of GNP incorporation within UHMWPE's crystalline structure. The virgin UHMWPE graphs and the (a) 1%(b) 15% (c) 20% of GNP embedded composites in the substrate(UHMWPE)are shown in Figure 22. The planes of orthorhombic crystal in UHMWPE are shown in each figure by two sharp arrow peaks at the angles of 21.5° and 24° respectively, in reference to the work of Wang et al. Phase analysis of unprocessed UHMWPE is shown in Figure 22. It features powerful, sharp peaks and a remarkable proportion of solid region. The results clearly show that the inclusion of graphene nanoplatelets (GNP) causes reduction in both reflection planes' crystallinity across the board for all samples. The Intensity droping reached to its apex.

The images also clearly show that it has a characteristic broad peak of graphene nanoplatelets(GNP)at an angle about 25.5°, despite some widening at Angle about 30° (figure 22) predicts the GNP composites' complete dispersion throughout the substrate. The sharp decline in 1% UHMWPE/GNP intensity relative to that of pure UHMWPE was another indication of complete dispersion of GNP. The loosening, breaking of the other substrate's connections and the progression towards a less crystalline phase are caused by GNP.[66 67]Table 1 lists the parameters for each sample that was gathered for x-ray analysis.

Table 1: Parameters from the X ray diffraction analysis

Sample	Angle i2θ	hkl	d(nm)	a(nm)	FWHM	Crystallite isize	Percentageicrystallinity(%)
P	22.51	120	0.5127	0.7294	0.7331	0.3228	47.18
	24.91	210	0.4718	0.7537			
PG_1	22.44	120	0.5141	0.7272	0.8685	0.3343	28.82
	24.81	210	0.4718	0.7566			
PG_5	22.45	120	0.5138	0.7267	0.8157	0.2971	38.05
	24.84	210	0.4728	0.7556			
PG_7	22.55	120	0.5119	0.7235	0.8970	0.2770	41.66
	24.92	210	0.4716	0.7532			
PG_{10}	22.50	120	0.5128	0.7251	0.8140	0.2975	42.28
	24.65	210	0.4758	0.7517			
PG_{15}	22.48	120	0.5132	0.7258	0.7385	0.3270	42.72
	24.89	210	0.4717	0.7541			
PG_{20}	22.52	120	0.5125	0.7244	0.7209	0.3272	44.37
	24.91	210	0.4717	0.7534			

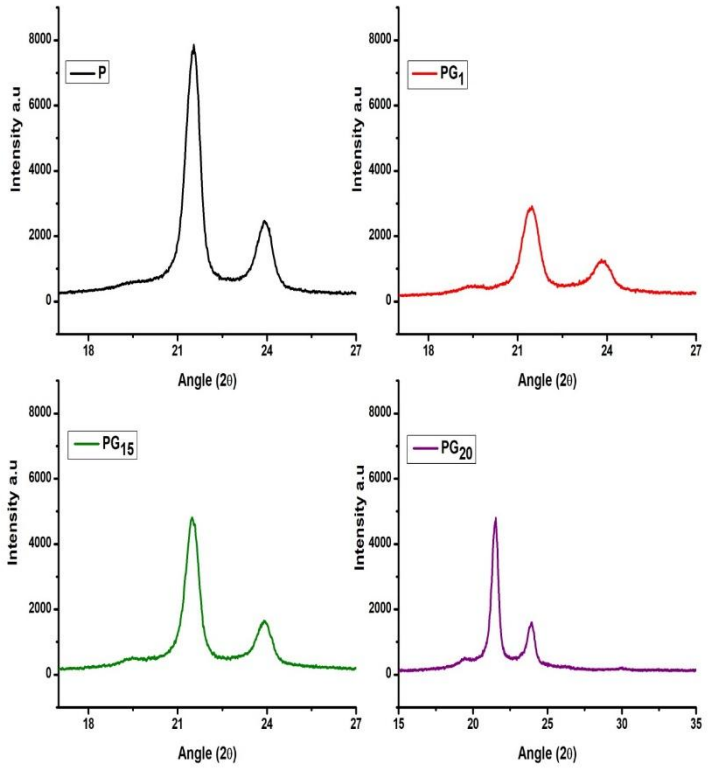

Figure 8: X-ray Diffracted Image of a Sample with Various Ratios

P is pure UHMWPE, PG1 is 1% GNP in UHMWPE, PG15 is 15% GNP in UHMWPE and PG20 is 20% UHMWPE.

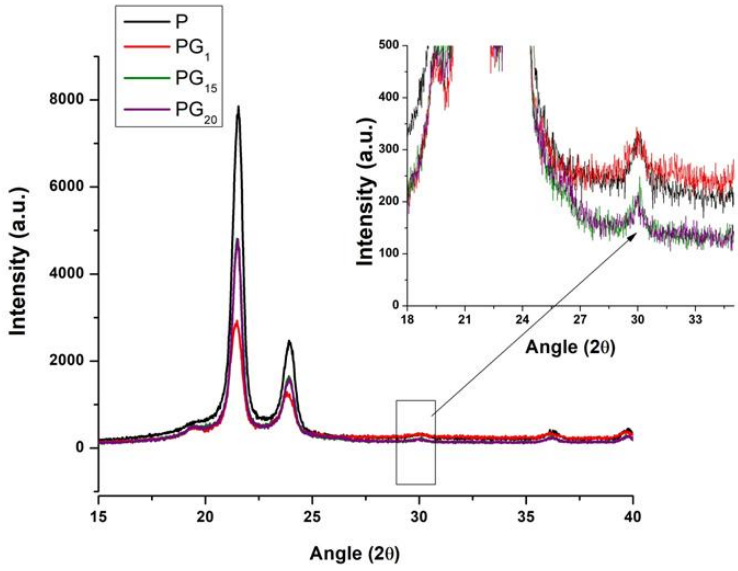

Figure 9 i: iBroadness iof I Graph eneinano particles

4.2 Thermoelectric Properties Analysis of UHMWPE/GNP Composites

4.2.1 Electrical conductivity

The GNP dispersion that creates a conductive network and transmits electrical energy explains conductivity in UHMWPE.The conductivity was unquestionably low when the GNP content was low and it grew as the GNP level increased. The present variation wasn't in the range of our device for pure, 1% and 5% GNP content in UHMWPE substrate. It demonstrated that the tiny conductivity and conductivity level were boosted by the addition of 10% GNP for the 7% content. Because of the increasing resistance in the polymer chain to the current and a decrease in the flexibility, mobility and plasticity of the polymer chains conductivity rose as GNP concentration increased.

Figure 24 displays the variation in conductivity as a function of temperature for graphene nano platelets concentrations of 7%, 10%, 15% and 20%. There is an erratic change in the current caused by a 7% increase in temperature. Electrical conductivity looks low for nonconductors and less than 10^{-7}mS/m, its range for 7% of the time between (10^{-8} and 10^{-7} mS/m), thus presumably it is not regarded as a conductor by us.Because GNP has a higher aspect ratio and is present in smaller amounts, it causes the UHMWPE links to break and forms a conductive channel. Temperature-related increases in conductivity happen gradually when GNP content approaches 10%.However, as the temperature rises, conductivity remains stable as graphene nanoplatelets starts to form in case of 15% and 20% concentration.

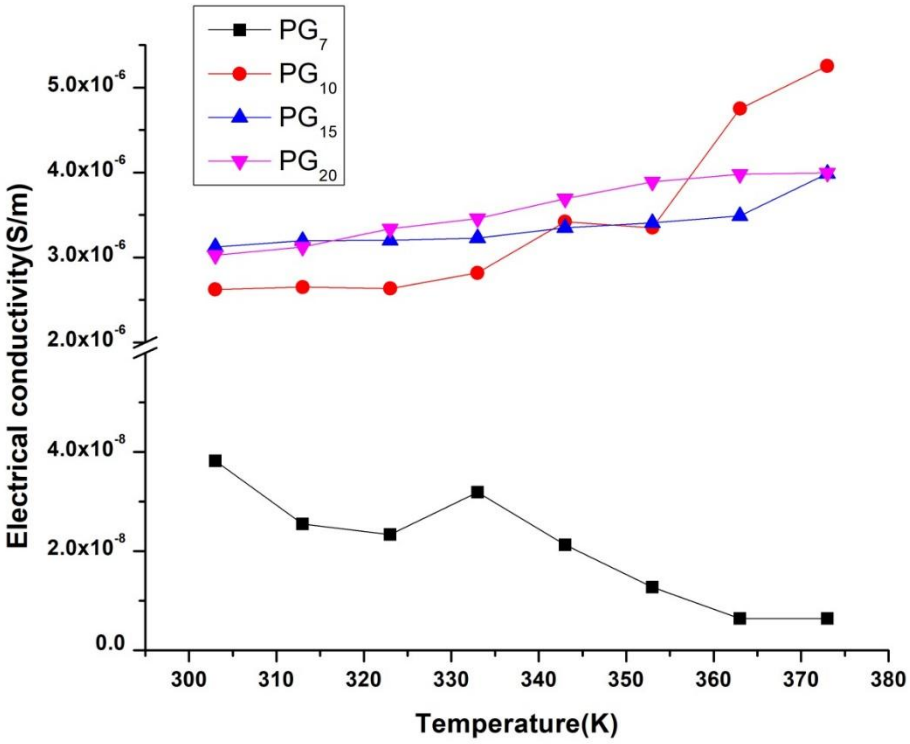

Figure 10: UHMWPE/GNP conductivity variation with temperature for 7%, 10%, 15%and 20% GNP content

4.2.2 Thermal conductivity

Figure 25 illustrates the connection among the thermal (conductivities, diffusivities) and heat volume is UHMWPE/GNP composites' capacities and GNP content in the UHMWPE substrate that is appropriate. With an increase in GNP content of up to 5%, thermal conductivity rises and the curve is linear. When adding another 10% of content, there is an even smaller decrease in electrical conductivity (approaching 0.51 W/mK) and when adding 15% and 20% of content, there is a very slight decline in the amount of content. This trend demonstrates that if we further raise the GNP content, it will have a negative impact on industrial output. For the most part phonons are seen of as thermal conductivity carriers.

The phonons in UHMWPE limit the thermal conductivity of UHMWPE/GNP composite materials which result in a significant rise in heat resistance as a result of the GNP boundaries. Decreased in conductivity is primary cause that the presence of graphene slows down heat diffusion and causes dislocations in atom rotation. Our composite's thermal diffusivity exhibited similar conduct to its thermal conductivity but at very low values. On the other hand, it differs greatly from both the trend of volumetric heat capacity and thermal conductivity, which have much larger values.

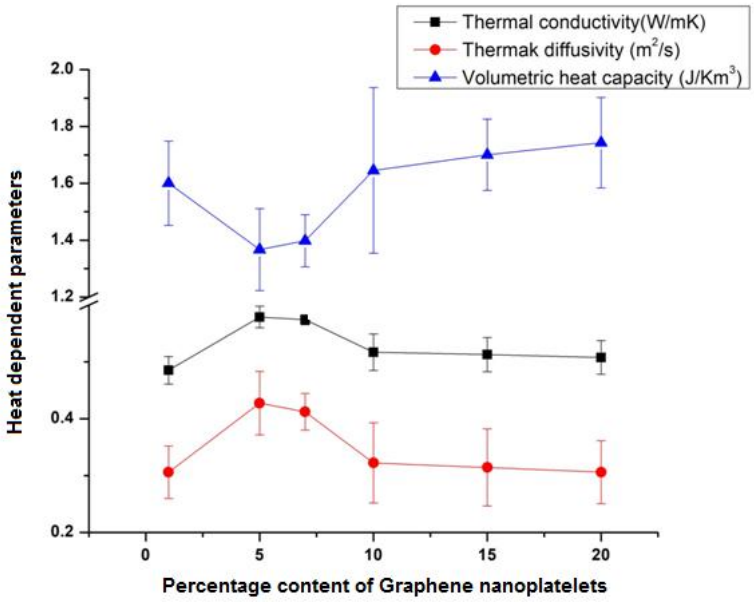

Figure 11: Variation of thermal conductivity, thermal diffusivity and volumetric heat capacity with graphene nanoplatelets content in UHMWPE

4.2.3 Seebeck coefficient

Following Section the voltage and temperature differential is used to determine the Seebeck coefficient. So that Seebeck's coefficient remains entirely unaffected by sample size and size, geometry is not a consideration.It is clear that pure electrical conductivity was discovered, 2% and 6% information is nonexistent. The voltage output to temperature difference ratio varies because electrical conductivity affects the Seebeck coefficient. As shown in Figure 25 that the As the amount of GNP increases, the Seebeck coefficients(7%, 10%, 15% and 20%)in a nanocomposite material raise and range from 170 to 235 V/K at temperature in UHMWPE.

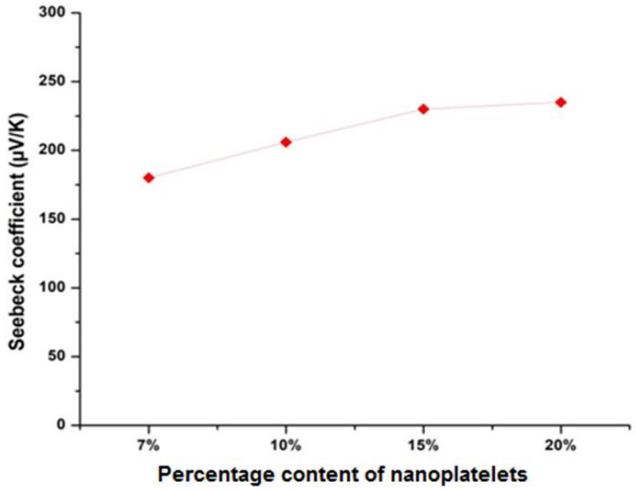

Figure 12:Variation of Seebeck coefficient with respect to increased content of graphene nanoplatelets.

4.2.4 Figure of merit

The figure of merit expresses the efficiency of the thermoelectric material. Figure 27 illustrates the reliance on the merit of UHMWPE/GNP nanocomposites with enhanced graphene nanoplatelets fractionation. The figure of merit demonstrates the quick increase in content from 7 to 10 percent.Even though Seebeck efficiency of 7 percent is much high, the electrical conductivity of this example is substantially lower in the range of 10^{-8} S/m, which is due to the lower efficiency of this example.The figure of merit demonstrates that larger values are reached when the respective electrical

and Seebeck coefficients grow with no change in thermal conductivities as graphene nanoplatelets concentrations rise from 10% to 15% and 20%.Additionally, these are values that aren't really appropriate for the frequent uses, although there may be other possibilities.

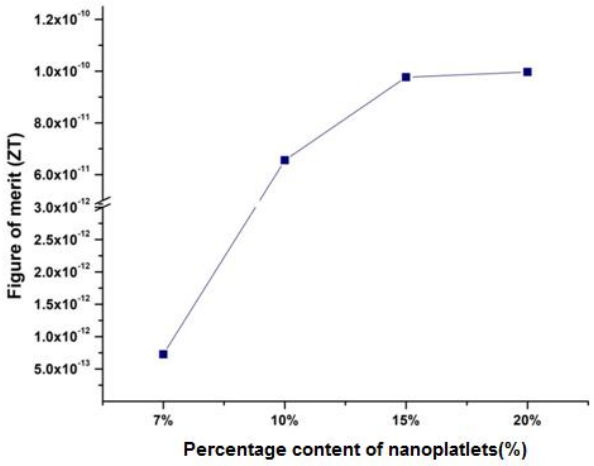

Figure 13: Reliance of figure of merit on graphene nanoplatelets content

Parameters upon which figure of merit depends at 303K are ilisted in itable 2.2

Table 2:Summary results for the thermoelectric characteristics of UHMWPE/GNPcomposites at ambient temperature.

Sample	Electrical iconductivity i	Seebeck icoefficient i	Power ifactor	Thermal iconductivity	Figureof imerit iZT
P	…	…	…	0.5852	…
PG_1	…	…	…	0.6789	…
PG_5	…	…	…	0.6741	…
PG_7	4.82167E-08	2.80E-04	2.23823E-15	0.6178	7.35967E-13
PG_{10}	3.62209E-06	3.06E-04	2.11272E-13	0.6152	6.65679E-11
PG_{15}	4.13E-06	3.30E-04	2.65287E-13	0.6139	9.86441E-11
PG_{20}	4.04E-06	3.35E-04	2.67057E-13	0.6088	9.86807E-11

5. CONCLUSION AND FURTHER RECOMMENDATION

In the recent decades, thermoelectric materials have shown to be a reliable source for energy production. The Seebeck coefficient is the most significant and critical parameter in terms of the thermoelectric properties of materials and polymer nanocomposites. In this study, graphene nano platelets (GNP) in percentages of 1, 5, 7, 10, 15 and 20 respectively, was mechanically mixed to create UHMWPE nano composites. The seebeck value for pure UHMWPE and UHMWPE/GNP nano composites with 1%, 5% and 10% weightage of GNP concentration is zero because of inherent insulating properties of UHMWPE. However, the Seebeck coefficient was found to be 180, 206, 230 and 235 V/K for composites with 7%, 10%, 15% and 20% weightage of GNP respectively. The exceptional ability to withstand heat and the conductive structure created by the GNPof the composites are credited with these higher levels of seeback coefficients. Because of the decreased charge carrier concentration in UHMWPE/GNP nano composites, the value of figure of merit and the power factor are minimal but the published results are nevertheless very encouraging for evaluating the composite material as a potential option for thermoelectric uses.

References

[1] N. Toshima, Recent progress of organic and hybrid thermo electric materials, Synth. Met. 225 (2017) 2073e2091.

[2] Q. Wei, M. Mukaida, K. Kirihara, Recent progress on PEDOT-based thermo-electric materials, Materials 8 (2015) 3e21.

[3] W. Shi, T. Zhao, J. Xi, Unravelling doping effects on PEDOT at the molecular level: from geometry to thermoelectric transport properties, J. Am. Chem. Soc.137 (2015) 12929e12938.

[4] A. Benchirouf, S. Palaniyappan, R. Ramalingame, Electrical properties of multi-walled carbon nanotubes/PEDOT: PSS nanocomposites thinfilms under temperature and humidity effects, Sensor. Actuator. B Chem. 224 (2016)344e350.

[5] H. Ju, J. Kim, Fabrication of conductive polymer/inorganic nano particles composite films: PEDOT: PSS with exfoliated tin selenide nanosheets for polymer-based thermo electric devices, Chem.Eng.J.297(2016)66e73.

[6] K. Zhang, S. Wang, X. Zhang, Thermoelectric performance of p-type nano-hybrids filled polymer composites, Nano Energy 13 (2015) 327

[7] L.Stepien,A.Roch,S.Schlaier,Investigationofthethermoelectricpowerfactorof KOH-treated PEDOT: PSS dispersions for printing applications, Energy Harvest. Syst. 1 (2015) 1e11.

[8] Z. Zhu, C. Liu, H. Shi, An effective approach to enhanced thermo electric properties of PEDOT: PSS films by a DES post-treatment, J. Polym. Sci. B Polym. Phys. 53 (12) (2015) 885e892.

[9] M. Culebras, C.M. Go´mez, A. Cantarero, Enhanced thermoelectric performanceofPEDOTwithdifferentcounter-ionsoptimizedbychemicalreduction, J.Mater.Chem.A2(2014)10109e10115.

[10] M. Hokazono, H. Anno, N. Toshima, Thermoelectric properties andthermalstability of PEDOT: PSSfilms on a polyimide substrate and application inflexible energy conversion devices, J. Electron. Mater. 43 (6) (2014)2196e2201.

[11] S.H. Lee, Y. Kim, J. Kim, Synthesis ofpolythiophene/poly(3,4-ethylenedioxythiophene) nanocomposites and their application in thermo-electric devices, J. Electron. Mater. 43 (2014) 3276e3282.

[12] H. Shi, C. Liu, J. Xu, Electrochemical fabrication and thermo electric performance of the PEDOT: PSS electrode based bilayered organic nanofilms, Int. J.Electrochem. Sci. 9 (2014) 7629e7643.

[13] L. Wang, F. Jiang, J. Xiong, Effects of second dopants on electrical conductivity and thermopower of poly (3,4 ethylenedioxy thiophene) :poly(-styrenesulfonate)-filledcarbonblack,Mater.Chem.Phys.153(2015)285e290.

[14]J. Park, A. Lee, Y. Yim, Electrical and thermal properties of PEDOT: PSSfilmsdopedwithcarbonnanotubes,Synth.Met.161(2011)523e527.

[15] Y.Y. Wang, K.F. Cai, S. Shen, In-situ fabrication and enhanced thermo electric properties of carbon nanotubes filled poly(3,4-ethylenedioxy thiophene) composites, Synth. Met. 209 (2015) 480e483.

[16] L.S. Vieira ,E.G.R.dos Anjos,G.E.A Verginio , I.C.Oyama, N.F.Braga,T.F da Silva, L.S.Montagna F.R

[17] Passador,2022,Nano Select , 3(2),248-260,

[18] A.P.B.Silva , L.S.Montagna, F.R.Passador , M.C.Rezende,A.P.Lemes,2021,EXPRESS polymer Letter,15(10),987-1003

[19] D.Markham,2000 ,Materials and Design , 21 , 45-50.